Molecular Biology of the Cell
Vol. 17, 3456–3468, August 2006

Rad4^{TopBP1}, a Scaffold Protein, Plays Separate Roles in DNA Damage and Replication Checkpoints and DNA Replication[D]

Lorena Taricani and Teresa S.F. Wang

Department of Pathology, Stanford University School of Medicine, Stanford, CA 94305-5324

Submitted January 23, 2006; Revised May 12, 2006; Accepted May 15, 2006
Monitoring Editor: Mark Solomon

Rad4^{TopBP1}, a BRCT domain protein, is required for both DNA replication and checkpoint responses. Little is known about how the multiple roles of Rad4^{TopBP1} are coordinated in maintaining genome integrity. We show here that Rad4^{TopBP1} of fission yeast physically interacts with the checkpoint sensor proteins, the replicative DNA polymerases, and a WD-repeat protein, Crb3. We identified four novel mutants to investigate how Rad4^{TopBP1} could have multiple roles in maintaining genomic integrity. A novel mutation in the third BRCT domain of *rad4$^{+TopBP1}$* abolishes DNA damage checkpoint response, but not DNA replication, replication checkpoint, and cell cycle progression. This mutant protein is able to associate with all three replicative polymerases and checkpoint proteins Rad3^{ATR}-Rad26^{ATRIP}, Hus1, Rad9, and Rad17 but has a compromised association with Crb3. Furthermore, the damaged-induced Rad9 phosphorylation is significantly reduced in this *rad4^{TopBP1}* mutant. Genetic and biochemical analyses suggest that Crb3 has a role in the maintenance of DNA damage checkpoint and influences the Rad4^{TopBP1} damage checkpoint function. Taken together, our data suggest that Rad4^{TopBP1} provides a scaffold to a large complex containing checkpoint and replication proteins thereby separately enforcing checkpoint responses to DNA damage and replication perturbations during the cell cycle.

INTRODUCTION

Eukaryotic cells have evolved a complex network of genomic surveillance mechanisms "checkpoints" to maintain genomic integrity in the face of various genomic insults during cell cycle progression. Checkpoint responses detect the genomic perturbations by sensor proteins, which then relay the signal to transducer proteins, and to effectors to transiently arrest the cell cycle (Nyberg *et al.*, 2002). Failure to enforce the correct checkpoint responses can result in the accumulation of mutations and chromosomal rearrangements, which are the hallmarks of cancer cells (Bakkenist and Kastan, 2004; Kastan and Bartek, 2004; Lukas and Bartek, 2004).

Rad4/Cut5 of fission yeast and its orthologues, budding yeast *DPB11*, *Drosophila* Mus101, and mammalian TopBP1, are essential for both DNA replication and checkpoint responses, giving them a unique role in genome maintenance (Saka and Yanagida, 1993; Saka *et al.*, 1994a, 1994b; Araki *et al.*, 1995; McFarlane *et al.*, 1997; Verkade and O'Connell, 1998; Makiniemi *et al.*, 2001; Harris *et al.*, 2003; Furuya *et al.*, 2004; Garcia *et al.*, 2005). Rad4/Cut5 (hereafter termed Rad4^{TopBP1}) in mouse and fission yeast is also involved in monitoring meiotic checkpoint (Perera *et al.*, 2004). Rad4^{TopBP1} of fission yeast contains four BRCT domains has been show to interact with a BRCT-repeat protein, Crb2, an adaptor for Chk1 activation, as well as a WD-repeat protein, Crb3, by two-hybrid criteria (Saka *et al.*, 1997; Garcia *et al.*, 2005). The fission yeast Crb3 is an ortholog of mammalian Wdr18 (Killian and Hubbard, 2004; NCBI, database). It is essential for viability of fission yeast although its physiological role is unknown (Saka *et al.*, 1997).

It is intriguing that Rad4^{TopBP1}, a single protein, is required for both DNA replication and checkpoint responses in genome maintenance. Despite numerous intense studies, the mechanism by which Rad4^{TopBP1} coordinates its multiple roles in maintaining genome integrity is unclear. Studies of Rad4^{TopBP1} of fission yeast have shown that phosphorylation of the checkpoint clamp component, Rad9, on Thr^{412} and Ser^{423} in response to damage promotes Rad9 protein to associate with two C-terminal BRCT domains of Rad4^{TopBP1}. This association is a prerequisite for activation of the Chk1 damage checkpoint but not the Cds1 replication checkpoint. Furthermore, Rad4^{TopBP1} is able to coprecipitate with Rad3^{ATR} when Rad9 is phosphorylated at Thr^{412} and Ser^{423}. The study suggests that phosphorylation of Rad9 at Thr^{412} and Ser^{423} coordinates the formation of an active checkpoint complex, which depends on the physical involvement of Rad4^{TopBP1} (Furuya *et al.*, 2004). Moreover, a recent study of Rad4^{TopBP1} of both *Xenopus* and human has shown that Rad4^{TopBP1} plays a critical role in the initiation of ATR-dependent checkpoint signaling processes (Kumagai *et al.*, 2006).

We show here that Rad4^{TopBP} physically associates with the checkpoint sensor proteins and the replicative DNA polymerases. We identified four novel mutants of *rad4$^{+TopBP1}$* to investigate how Rad4^{TopBP1} coordinates its multiple roles to maintain genomic integrity. A detailed analysis of one mutant having a mutation in the third BRCT motif (R3) indicates that the role of Rad4^{TopBP} in checkpoint responses to DNA damage can be separated from the checkpoint response to replication perturbation and from its role in DNA replication and cell cycle

This article was published online ahead of print in *MBC in Press* (http://www.molbiolcell.org/cgi/doi/10.1091/mbc.E06–01–0056) on May 24, 2006.

[D] The online version of this article contains supplemental material at *MBC Online* (http://www.molbiolcell.org).

Address correspondence to: Teresa S.F. Wang (tswang@stanford.edu).

progression. Furthermore, genetic and biochemical analyses suggest that Crb3 transiently associates with Rad4^{TopBP1}; Crb3 has a role in maintaining the DNA damage checkpoint and seems to influence the DNA damage checkpoint function of Rad4^{TopBP1}. Taken together, our results suggest that Rad4^{TopBP1} functions as a scaffold in a large protein complex containing both checkpoint proteins and replication proteins to selectively enforce checkpoint response to DNA damage or replication perturbation, or DNA replication in order to maintain genomic integrity during the cell cycle.

MATERIALS AND METHODS

Strains and Media

Schizosaccharomyces pombe strains were grown in YES or EMM medium containing nutritional supplements as necessary. Standard genetic methods, molecular biological techniques, and generation of tagged strains were as described in Moreno *et al.* (1991) and Bahler *et al.* (1998). GFP(S65T) tag was constructed to the C-terminus of *rad4$^{+TopBP1}$* and *rad4-c11^{TopBP1}* at its genomic locus, and GFP-tagged Rad4^{TopBP1} and Rad4-c11^{TopBP1} are nuclear proteins (unpublished data). Cells containing GFP epitope–tagged *rad4$^{+TopBP1}$* (*rad4$^{+TopBP1}$:GFP*) and *rad4-c11^{TopBP1}* (*rad4-c11^{TopBP1}:GFP*) have phenotype and properties identical to that of the wild-type and *rad4-c11^{TopBP1}* cells, respectively (Supplementary Figure 1). Diploid strain Δ*crb3*/+ with one copy of the *crb3^{+}* deleted was generated using PCR-mediated gene disruption (Bahler *et al.*, 1998). Other diploid strains were generated by protoplast fusions or by crossing two homothallic diploid strains with complementing *ade6* markers. The *ade^{+}* diploids are selected and analyzed by PCR and confirmed by sequencing. All strains used in this study are listed in Supplementary Tables 1 and 2.

Synchronization of Cells by cdc25 Block Release

Synchronization of G2 phase of cells harboring *cdc25-22* mutation was performed by shifting cultures grown to early log phase at 25°C for 4 h to 36.5°C. Cells were then released into the cell cycle at 25°C with or without 30 μM camptothecin (CPT). To assess checkpoint deficiency after exposure to CPT, cells were scored for septation every 30 min.

Preparation of Protein Extract and Immunoprecipitation and Immunoblotting of Rad4^{TopBP1}:GFP

Cells were harvested by centrifugation and washed once with ice-cold stop buffer (150 mM NaCl, 50 mM NaF, 10 mM EDTA, 1 mM NaN_3, pH 8.0) and once with LT500 lysis buffer (25 mM Tris-HCl, pH 7.4, 500 mM NaCl, 1 mM EDTA, 10% glycerol, 10 mM β-mercapthoethanol). The cells were resuspended in LT500 lysis buffer supplemented with 1 mM phenylmethylsulfonyl fluoride (PMSF) and 2× protease inhibitors (Roche Molecular Biochemicals, Indianapolis, IN) and frozen as pellets by dropping the cell suspension into liquid nitrogen. The frozen cell pellets were broken in the dry ice powder using a coffee grinder. The homogenate was resuspended in LT300 lysis buffer (25 mM Tris-HCl, pH 7.4, 300 mM NaCl, 1 mM EDTA, 10% glycerol, 0.1% Nonidet P-40, 10 mM β-mercapthoethanol, and 1 mM PMSF, supplemented with complete protease inhibitors; Roche Molecular Biochemicals), vortexed, sonicated, treated with DNAse I (Invitrogen, Carlsbad, CA), and then centrifuged to prepare a cleared whole-cell extract. Protein concentration was determined using the Bio-Rad protein assay (Richmond, CA).

Three milligrams of total protein was diluted to 300 μl with LT300 lysis buffer and incubated with mouse anti-GFP monoclonal antibody (Roche Molecular Biochemicals) at 4°C for 2 h. Protein G plus protein A-Agarose beads (50 μl, Oncogene Research Products, Boston, MA) were added and incubated at 4°C for 1 h. Immunoprecipitates were washed four times with LT300 lysis buffer and resuspended in 30 μl of 2× SDS loading buffer. For immunoblot analysis, 40–60 μg of total protein was loaded for detection of protein in input lysates. Ten micrograms of total immunoprecipitated materials was used in SDS-PAGE for detection of immunoprecipitation, and 20 μg was used for detection of the coimmunoprecipitation. Extracts were separated on SDS-PAGE and transferred to PVDF membrane (Bio-Rad). Two protein bands marked with asterisks were Rad4^{TopBP1}:GFP in full-length (100 kDa) and in N-terminal truncated (93-kDa) in all immunoprecipitates. Immunoblots were probed with appropriate antibodies: mouse anti-GFP antibody (1:1000; Roche Molecular Biochemicals) for Rad4^{TopBP1}; mouse anti-M2 FLAG antibody (1:1000; Sigma) for FLAG-tagged polymerases δ and ε; mouse anti-myc (9E10; 1:2000) for myc-tagged Rad3^{ATR}, Hus1, and Rad17; and chicken B18 anti-polα (1:1000) for polymerase α (Park *et al.*, 1993). Immunoreactive bands were revealed with HRP-conjugated secondary goat anti-mouse, anti-rabbit IgG antibody (1:10,000), or anti-chicken IgG antibody (1:5000; New England BioLabs, Beverly, MA) and the luminol-based ECL detection kit (Perkin Elmer-Cetus, Norwalk, CT). Immunoprecipitation of Rad26^{ATRIP} was performed by rabbit anti-Rad26^{ATRIP} (1:1000) and probed the immunoblot by anti-GFP (1:1000) for Rad4^{TopBP1}:GFP or Rad4-c11^{TopBP1}:GFP.

Cds1 Immunoprecipitation and Kinase Assay

Immunoprecipitation of Cds1 protein and Cds1 kinase activity were performed as described (Lindsay *et al.*, 1998).

Chk1 Immunoprecipitation

Protein extraction was performed with glass beads in LT300 lysis buffer using FastPrep (BIO 101, Carlsbad, CA) vortexing machine. For Chk1 immunoprecipitation (IP) in the *rad4$^{+TopBP1}$*:GFP cells and mutant *rad4-c11^{TopBP1}*:GFP cells, 5 mg of soluble protein was added to 100 μl of anti-HA (3F10) affinity matrix (Roche Molecular Biochemicals) and incubated at 4°C with rocking for 5 h. Immunoprecipitates were washed four times with LT300 lysis buffer and resuspended in 2× SDS gel loading buffer. Ten microliters of each IP were separated on 8% SDS-PAGE, transferred to PVDF membrane (Bio-Rad), and detected by anti-HA 12CA5 (1:500; Roche Molecular Biochemicals).

DAPI Staining

Cells were collected and fixed in 100% methanol at −20°C for at least 20 min. Cells were then washed three times in 1× PEM buffer (Sawin and Nurse, 1998), resuspended in 20–50 μl 1× PEM, and stained with 1 μg/ml DAPI. All images were photographed with a Nikon epifluorescence microscope (Melville, NY).

Two-Hybrid Assay

The full-length *crb3^{+}* and *rad9^{+}* was fused to the 3′ end of the LexA DNA-binding domain in pEG202 (Gyuris *et al.*, 1993) to generate a BamHI/NotI *crb3^{+}* and *rad9^{+}* fragment by PCR and to clone into the BamHI/NotI sites to yield the bait plasmids. The wild-type R3 and mutant R3-c11 domain of *rad4^{TopBP1}* was fused to LexA DNA-binding domain in pEG202 by first generating a BamHI/NotI R3 and R3-c11 *rad4^{TopBP1}* fragment by PCR and then cloning into the BamHI/NotI sites, to yield the bait plasmid. The full-length *rad4$^{+TopBP1}$*, *cds1^{+}*, *chk1^{+}*, and *crb3^{+}* were independently constructed to the 3′end of the *GAL4* transcriptional activation domain and cloned into the EcoRI/XhoI sites. *rad4^{TopBP1}* fragments deleted for the first two BRCT domains (R1 and R2) region, Δ*R1R2rad4^{TopBP1}* and Δ*R1R2rad4-c11^{TopBP1}*, which contains a mutation in the R3 region, were independently fused to the 3′ end of the *GAL4* transcriptional activation domain and cloned into the EcoRI/XhoI sites. The two-hybrid experiments were performed with *S. cerevisiae* strain Y1003. Activities of β-galactosidase were expressed in Miller units as the mean of six independent determinations (±SD).

RESULTS

Characterization of rad4^{TopBP1} Mutants

We devised a genetic screen using *cdc20-M10* (a *polε* mutant) to identify genetic elements that are involved in activating Chk1 after early S-phase arrest (Griffiths *et al.*, 2000). Four novel *rad4$^{+TopBP1}$* mutants were isolated by this screen among many of the checkpoint mutants. All four novel *rad4^{TopBP1}* mutants reside in the BRCT domains of Rad4^{TopBP1} (Figure 1A). One mutant, *rad4-c23^{TopBP1}*, contains an His^{46} to Tyr (H46Y) substitution residing in the first BRCT domain (R1). This mutation is immediately adjacent to the previously identified, and well-documented, thermosensitive *rad4-116^{TopBP1}* mutant, which contains a Thr^{45} to Met (T45M) substitution and is defective in checkpoint responses to damage and replication perturbations at its restrictive temperature (Saka *et al.*, 1994a, 1997; Harris *et al.*, 2003). Interestingly, *rad4-c23^{TopBP1}* is not thermosensitive (Figure 1B). Two new mutants, *rad4-m15^{TopBP1}* and *rad4-c17^{TopBP1}*, contain A155T and S171N substitutions, respectively, within the second BRCT domain (R2). *rad4-c17^{TopBP1}* is the only temperature-sensitive mutant isolated (Figure 1, A and B). One mutant, *rad4-c11^{TopBP}*, contains an E368K substitution within the third BRCT domain (R3; Figure 1A). The *rad4-c11^{TopBP1}* mutation is localized within the conserved motif (consensus W-X-X-X-C/S) found in all BRCT domains.

These novel *rad4^{TopBP1}* mutants were tested for their sensitivity to different genotoxic agents. The *rad4^{TopBP1}* mutants exhibit varying levels of sensitivity to UV with

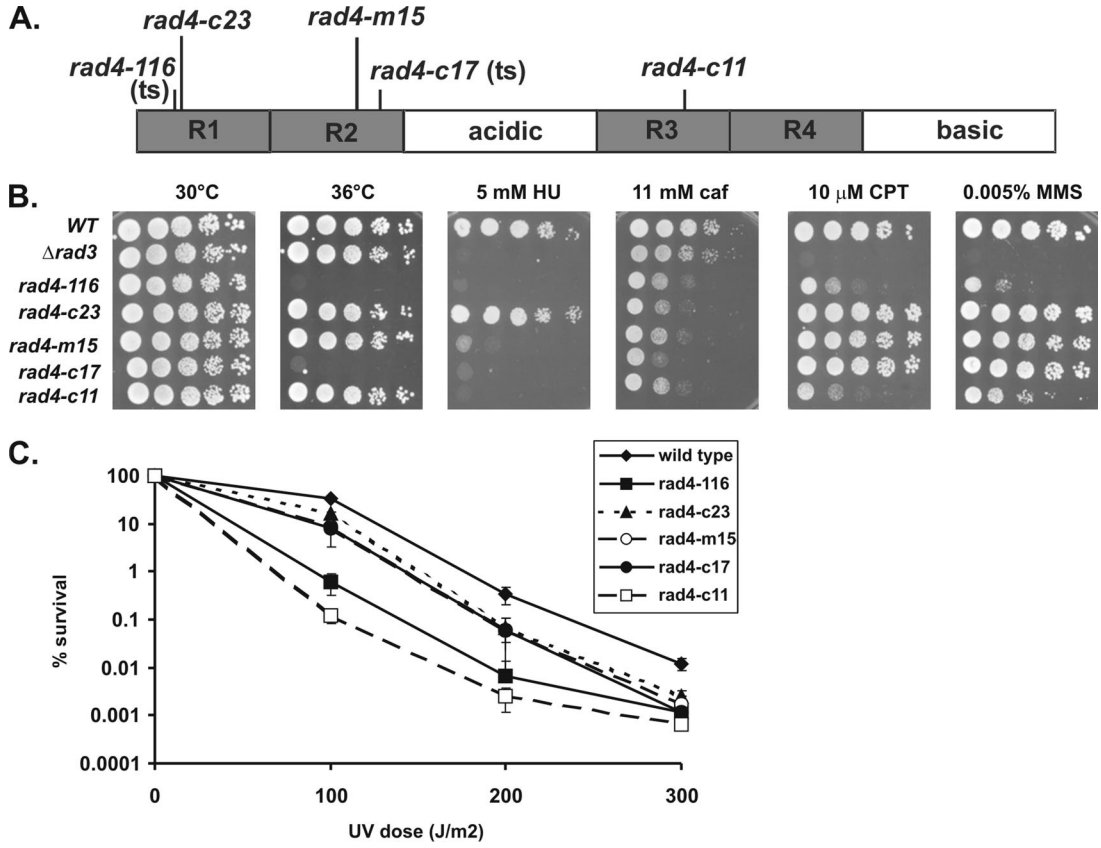

Figure 1. Characterization of novel *rad4*^{TopBP1} mutants. (A) Schematic locations of the novel *rad4*^{TopBP1} mutations. Rad4^{TopBP1} consists of four BRCT domains (R1, R2, R3, and R4) and two hydrophilic (acidic and basic) domains. Locations of the novel mutants and the previously characterized mutant *rad4-116*^{TopBP1} in each BRCT domain are marked. (B) Sensitivities of the *rad4*^{TopBP1} mutants to genotoxic agents. Cells were cultured to log phase, and then 10-fold serial dilutions of 1×10^7 cells were spotted onto YES plates or YES plates with 5 mM HU, 11 mM caffeine, 10 μM CPT, or 0.005% MMS and incubated at 30°C for 3 d. (C) UV sensitivity of *rad4*^{TopBP1} mutants. Wild-type and *rad4*^{TopBP1} mutants were grown in YES to early log phase, and then >1000 cells were plated in triplicate on YES plates. Cells were irradiated with the indicated doses of UV and incubated at 25°C for 5 d. Data shown represents the average results of three independent experiments.

rad4-c11^{TopBP1} exhibiting a slightly higher UV sensitivity than *rad4-116*^{TopBP1} (Figure 1C; Saka and Yanagida, 1993; McFarlane *et al.*, 1997). *rad4-c11*^{TopBP1} and *rad4-116*^{TopBP1} exhibit similar sensitivity to hydroxyurea (HU), caffeine (caf), CPT, and methyl methanesulfonate (MMS) at 30°C (Figure 1B). In contrast to *rad4-116*^{TopBP1}, mutant *rad4-c23*^{TopBP1}, containing a mutation immediately adjacent to *rad4-116*^{TopBP1}, is only sensitive to caffeine and mildly sensitive to UV (Figure 1, B and C). *rad4-116*^{TopBP1}, *rad4-m15*^{TopBP1}, and *rad4-c11*^{TopBP1} are all sensitive to γ-radiation, whereas *rad4-c23*^{TopBP1} and *rad4-c17*^{TopBP1} are not γ-radiation sensitive (unpublished data). These results indicate that mutations in different alleles, even adjacent alleles in the same BRCT-domain, can induce disparate phenotypes in cells.

Mutation in rad4-c11^{TopBP1} *Abolishes Cells' Chk1 Checkpoint Responses to DNA Damage But Not the Cds1 Response to Replication Perturbation*

Rad4^{TopBP1} is required to enforce checkpoint responses to replication stress and DNA damage (Garcia *et al.*, 2005). We thus analyzed whether the new *rad4*^{TopBP1} mutants could compromise replication checkpoint by analyzing the Cds1 kinase activation in response to HU treatment. The Cds1 kinase activity in the HU-treated thermosensitive mutants *rad4-116*^{TopBP1} and *rad4-c17*^{TopBP1} was activated to a comparable extent as in wild-type cells at the permissive temperature of 26°C and at the semipermissive temperature of 32°C (Figure 2A). As expected, Cds1 kinase activity was dramatically reduced in *rad4-116*^{TopBP1} and reduced to a lesser extent in *rad4-c17*^{TopBP1} at the restrictive temperature of 36°C (Figure 2A). The non–temperature-sensitive mutants *rad4-c23*^{TopBP1}, *rad4-m15*^{TopBP1}, and *rad4-c11*^{TopBP1} are all proficient in Cds1 kinase activation (Figure 2B).

We next tested whether the *rad4*^{TopBP1} mutants were compromised for their response to DNA damage induced by CPT treatment by assessing the phosphorylation of Chk1 protein. CPT induces DNA damage by inhibiting the religation step of the topoisomerase I reaction (Porter and Champoux, 1989). When the advancing replication fork encounters the CPT-stabilized topoisomerase I–DNA complex, the replication fork would collapse. Chk1 phosphorylation can be detected by the HA-epitope–tagged Chk1 protein's retarded mobility in gel electrophoresis (Walworth and Bernards, 1996). As expected, the temperature-sensitive mutant, *rad4-116*^{TopBP1} showed severely compromised Chk1 phosphorylation at 30°C (Figure 2C). Surprisingly, the temperature-sensitive mutant *rad4-c17*^{TopBP1} and mutant *rad4-c23*^{TopBP1} were proficient in Chk1 activation, showing levels of Chk1 phosphorylation similar to that in the non–temperature-sensitive mutant *rad4-m15*^{TopBP1} and wild-type cells at 30°C (Figure 2C). Significantly, no Chk1 phosphorylation was detected in

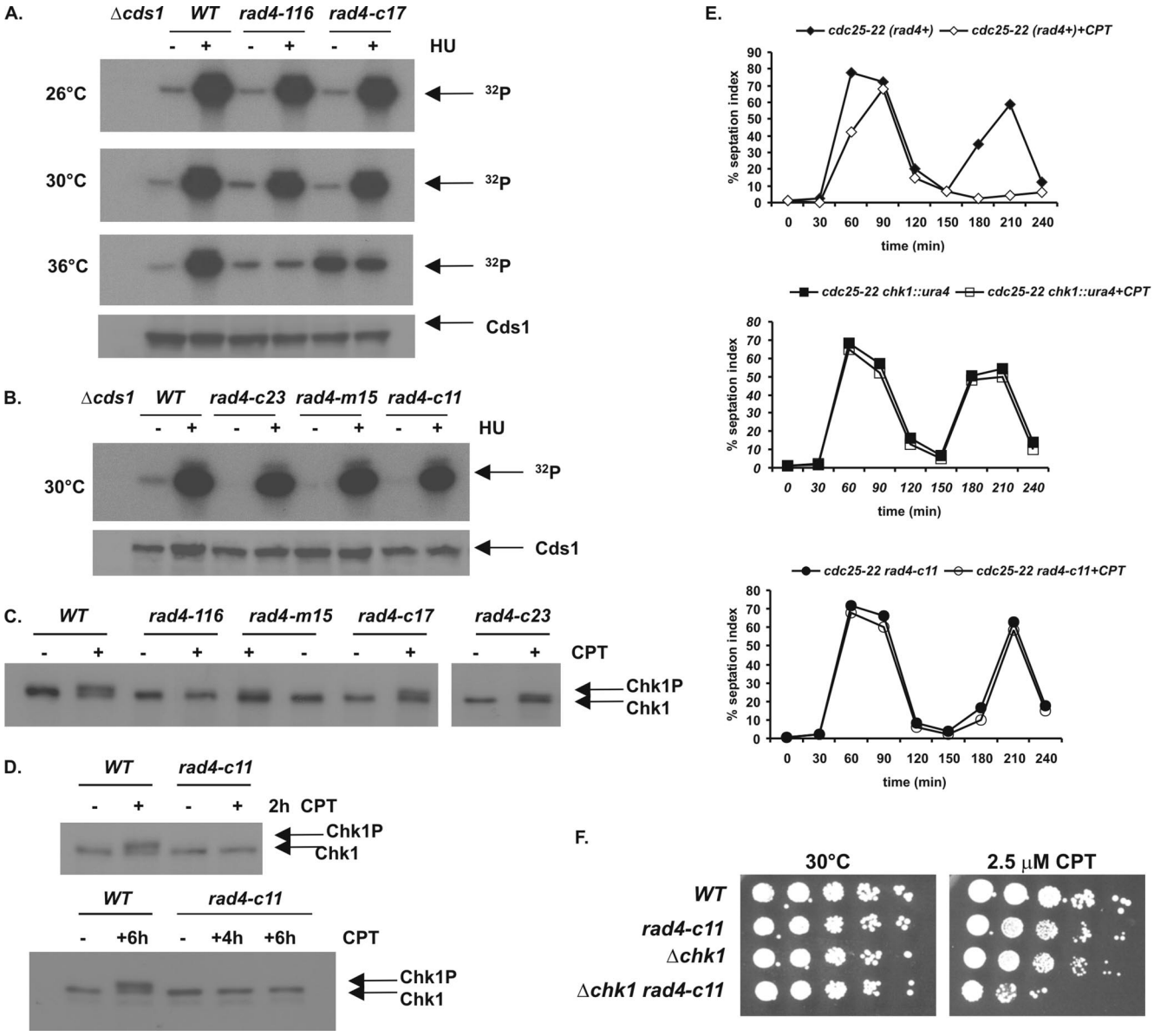

Figure 2. Activation of Cds1 and Chk1 kinases in *rad4^{TopBP1}* mutants. Cds1 kinase assays were performed as described in *Material and Methods.* Chk1 activation was measured by the phosphorylation-dependent mobility shift of Chk1 protein in *rad4$^{+TopBP1}$:GFP* and *rad4^{TopBP1}:GFP* mutants cells containing an integrated HA-tagged *chk1^{+}* as described in *Materials and Methods.* (A) Cds1 kinase activity of the thermosensitive mutants. (B) Cds1 kinase activity of the nonthermosensitive mutants. (C) Chk1 phosphorylation of the thermosensitive mutants, *rad4-116^{TopBP1}* and *rad4-c17^{TopBP1}* and nonthermosensitive mutants *rad4-m15^{TopBP1}* and *rad4-c23^{TopBP1}*. (D) Mutation in *rad4-c11^{TopBP1}* abolishes Chk1 activation. Mutant *rad4-c11^{TopBP1}* cells were treated with CPT for 2 h (top panel) and 4 h and 6 h (bottom panel). (E) *rad4-c11^{TopBP1}* mutant is defective in delay of mitotic entry in response to damage. Cells were synchronized by *cdc25-22* block and release and then treated with or without 30 μM of CPT. The synchronous *cdc25-22 rad4$^{+TopBP1}$* (top panel), *cdc25-22* Δ*chk1* (middle panel), and *cdc25-22 rad4-c11^{TopBP1}* (bottom panel) cells were scored for septation index at 30-min intervals. Solid symbols represent cells not treated with CPT; open symbols are cells treated CPT. (F) Deletion of *chk1^{+}* in *rad4-c11^{TopBP1}* has a synergistic effect on the cells' sensitivity to chronic CPT treatment. Cells were cultured to log phase and then 10-fold serial dilutions of 1×10^7 cells were spotted onto YES plates or YES plates with 2.5 μM CPT and incubated at 30°C for 3 d.

rad4-c11^{TopBP1} after 2 h of CPT treatment (Figure 2D, top panel). It is possible that the failure of Chk1 activation in *rad4-c11^{TopBP1}* is a temporal phenomenon and that the Chk1 activation is able to recover after prolong CPT treatment. To test this possibility, we analyzed Chk1 phosphorylation in *rad4-c11^{TopBP1}* after 4 and 6 h of CPT treatment. As shown in Figure 2D, bottom panel, *rad4-c11^{TopBP1}* failed to activate Chk1 phosphorylation throughout 6 h of CPT treatment. These results indicate that the mutation in *rad4-c11^{TopBP1}* causes an irreversible defect in Chk1 DNA damage checkpoint.

To ensure that mutation in *rad4-c11^{TopBP1}* compromises the Chk1-mediated G2/M phase checkpoint, we analyzed the kinetics of mitotic entry of *rad4-c11^{TopBP1}* cells. Mutant *rad4-c11^{TopBP1}* was constructed in *cdc25-22* background and synchronized by *cdc25-22* block at G2 and release. The per-

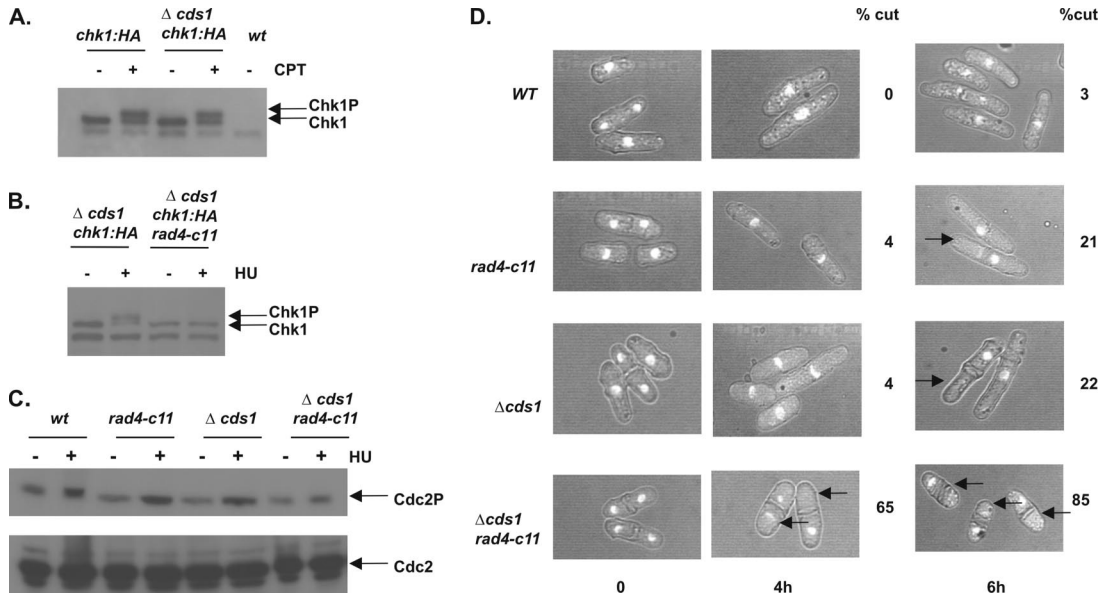

Figure 3. Mutations in *rad4-c11*^{TopBP1} abolish Chk1 activation in Δ*cds1* cells. (A) The Chk1 phosphorylation was assayed in *chk1:HA* and Δ*cds1 chk1:HA* mutant cells that were incubated with 30 μM CPT for 2 h at 30°C. (B) Cells with mutation in *rad4-c11*^{TopBP1} fail to activate Chk1 in the absence of *cds1*$^{+}$. *chk1:HA*, Δ*cds1 chk1:HA*, and Δ*cds1 chk1:HA rad4-c11*^{TopBP1} strains were incubated with 12 mM HU for 4 h at 30°C. Cell extracts were examined for phosphorylation dependent mobility shift of Chk1 in response to HU-induced damage in the absence of functional Cds1. (C) Phosphorylation of Cdc2 in HU-treated Δ*cds1 rad4-c11*^{TopBP1} double mutant is compromised. Wild-type *rad4*$^{+TopBP1}$ and mutants, *rad4-c11*^{TopBP1}, Δ*cds1*, and Δ*cds1 rad4-c11*^{TopBP1} cells were grown in YES media in the presence of 12 mM HU for the 4 h at 30°C and examined for Cdc2 phosphorylation levels. Cdc2 (PSTAIRE) was used as a loading control. (D) Deletion of *cds1*$^{+}$ in *rad4-c11*^{TopBP1} induces mitotic catastrophic phenotype in response to HU-induced damage. Wild-type, *rad4-c11*^{TopBP1}, Δ*cds1*, and Δ*cds1 rad4-c11*^{TopBP1} cells were grown in YES media in the presence of 12 mM HU for the indicated times at 30°C, fixed, and then stained with DAPI to determine % *cut* phenotype. Percentage *cut* phenotype represents the average result of two independent experiments of counting 300 cells. Arrows indicate cells with abnormal nucleus.

cent of cells entering mitosis upon CPT treatment was measured by septation index and compared with that of *cdc25-22* cells with wild-type *rad4*$^{+TopBP1}$ and double mutant Δ*chk1 cdc25-22*. As expected, cells with mutation in the *rad4-c11*^{TopBP1} or deletion of *chk1*$^{+}$ did not delay the mitotic entry in response to CPT treatment, whereas cells with *rad4*$^{+TopBP1}$ did not enter mitosis after CPT treatment (Figure 2E). We further tested the effect of deletion of *chk1*$^{+}$ in *rad4-c11*^{TopBP1} after chronic exposure to CPT on solid media. After chronic exposure to 2.5 μM CPT, the two single mutants exhibited similar viability. Interestingly, deletion of *chk1*$^{+}$ in *rad4-c11*^{TopBP1} had a synergistic effect on the double mutant's viability (Figure 2F). This result suggests that chronic exposure of *rad4-c11*^{TopBP1} to CPT may compromise another damage response pathway in addition to the response that activates Chk1 upon acute CPT treatment (Figure 2, A–E). These results support the notion that cellular responses to acute and chronic DNA damage are different and underscore the importance of the multiple roles of Rad4^{TopBP1} in genome maintenance.

Chk1 is not only activated in response to replication fork collapse induced by CPT (Figure 3A) but also by HU in the absence of Cds1 (Figure 3B; Boddy *et al.*, 1998; Lindsay *et al.*, 1998). To further determine whether the *rad4-c11*^{TopBP1} mutant is also defective in Chk1 activation in response to DNA damage caused by HU-induced replication fork stalling in the absence of Cds1, we created a mutant strain Δ*cds1 rad4-c11*^{TopBP1}*chk1:HA* to assess the phosphorylation of Chk1 protein in response to HU treatment. On HU treatment, Chk1 was activated in the Δ*cds1 chk1:HA* strain (Figure 3B). In contrast, no Chk1 phosphorylation was observed in the Δ*cds1 rad4-c11*^{TopBP1} *chk1:HA* strain after HU treatment (Figure 3B). Furthermore, upon HU treatment, only the Δ*cds1 rad4-c11*^{TopBP1} double mutant, deficient in both *cds1*$^{+}$ and *chk1*$^{+}$ activation, exhibited a reduced level of Cdc2 phosphorylation (Figure 3C). These results indicate that in the Δ*cds1 rad4-c11*^{TopBP1} double mutant, the Chk1-mediated mitotic checkpoint in response to HU treatment is abolished. Thus, *rad4-c11*^{TopBP1} mutant has a defective Chk1 activation in response to HU-treated Δ*cds1* cells.

To further ascertain that the mutation in *rad4-c11*^{TopBP1} abolishes activation of Chk1 in response to replication fork collapse, we quantified cells exhibiting mitotic catastrophic phenotype after HU treatment in liquid culture. After 4 h of HU treatment, wild-type, Δ*cds1,* and *rad4-c11*^{TopBP1} cells underwent checkpoint arrest, exhibiting an elongated *cdc* phenotype, with ~4% of *rad4-c11*^{TopBP1} and Δ*cds1* cells also exhibited the mitotic catastrophic *cut* phenotype. The *rad4-c11*^{TopBP1} mutant with intact *cds1*$^{+}$ activates Cds1 kinase, whereas Δ*cds1* mutant with intact *chk1*$^{+}$ activates Chk1 kinase in response to replication block induced by HU treatment, and thus both exhibit *cdc* phenotype (Figure 3D). In striking contrast, 65% of the double mutant Δ*cds1 rad4-c11*^{TopBP1} cells exhibited the *cut* phenotype after 4 h of HU treatment. After 6 h, the percentage of *cut* phenotype in *rad4-c11*^{TopBP1} and Δ*cds1* increased to 21–22%, and the *cut* phenotype in Δ*cds1 rad4-c11*^{TopBP1} double mutant increased to 85% (Figure 3D), similar to the HU-treated Δ*cds1* Δ*chk1* or Δ*rad3* cells. Taken together, these biochemical and genetic results unequivocally demonstrate that *rad4-c11*^{TopBP1}, a novel mutant of *rad4*^{TopBP1}, is indeed specifically defective in Chk1-mediated checkpoint response.

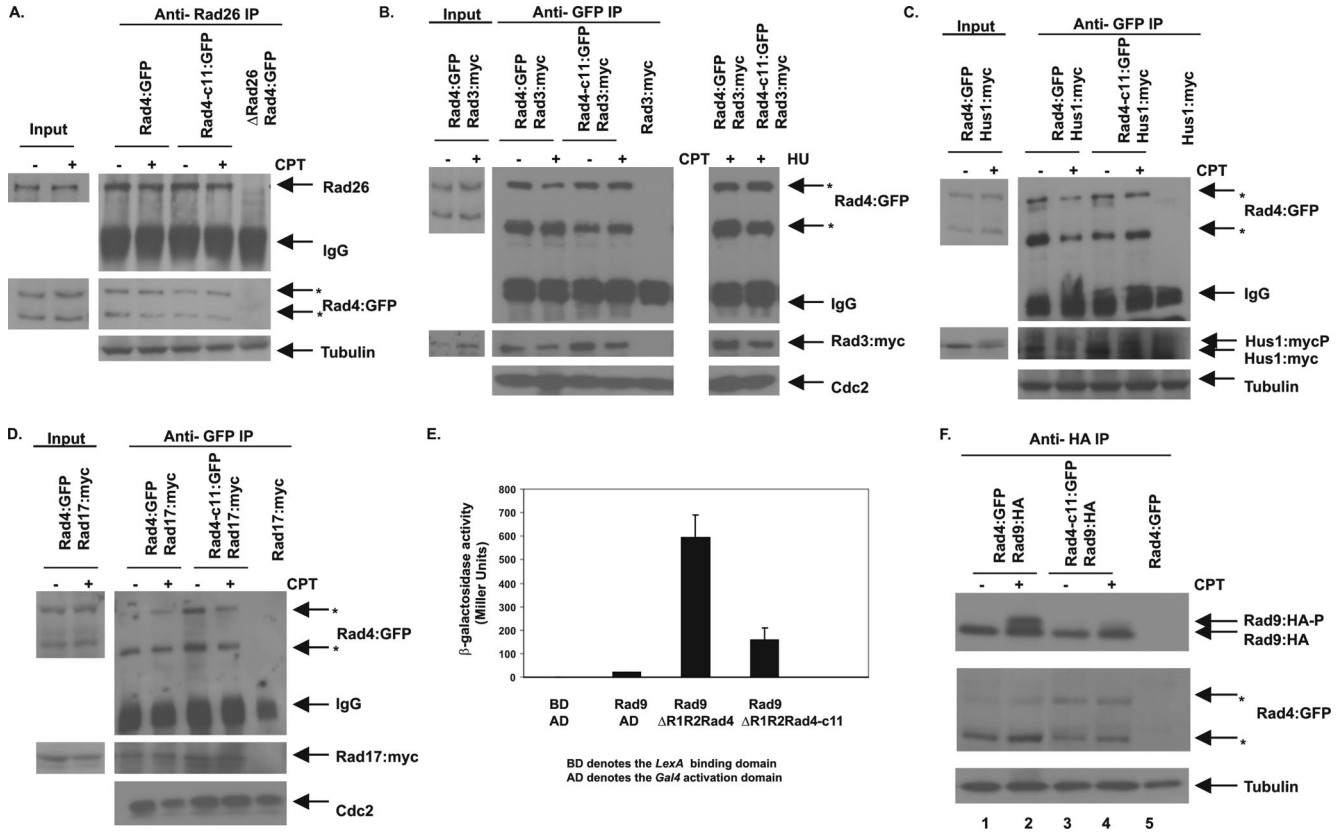

Figure 4. Rad4^{TopBP1} physically associates with checkpoint sensor proteins. (A) Coprecipitation of Rad4^{TopBP1}:GFP or Rad4-c11^{TopBP1}:GFP proteins with Rad26^{ATRIP}. (B) Coprecipitation of Rad4^{TopBP1}:GFP or Rad4-c11^{TopBP1}:GFP with Rad3^{ATR}:myc from extracts of *rad4$^{+TopBP1}$:GFP rad3^{+ATR}:myc* cell or *rad4-c11^{TopBP1}:GFP rad3^{+ATR}:myc* cells treated with CPT or HU. (C) Coprecipitation of Hus1:myc with Rad4^{TopBP1}:GFP or Rad4-c11^{TopBP1}:GFP from extracts of *rad4$^{+TopBP1}$:GFP hus1^{+}:myc* or *rad4-c11^{TopBP1}:GFP hus1^{+}:myc* cells. (D) Coprecipitation of Rad17:myc with Rad4^{TopBP1}:GFP or Rad4-c11^{TopBP1}:GFP from extracts of *rad4$^{+TopBP1}$:GFP rad17^{+}:myc* or *rad4-c11^{TopBP1}:GFP rad17^{+}:myc* cells. Cell cultures were grown in YES media in the absence (−CPT) or presence (+CPT) of 30 μM CPT for 2 h at 30°C. Immunoprecipitations were performed as described in *Materials and Methods.* (E) Rad9 interacts with Rad4^{TopBP1} and Rad4-c11^{TopBP1} by two-hybrid assay. (F) Rad4^{TopBP1} and Rad4-c11^{TopBP1} physically associate with Rad9 in vivo. Rad9:HA was immunoprecipitated by anti-HA (3F10) affinity matrix from extracts of *rad9:HA rad4$^{+TopBP1}$:GFP* or *rad9:HA rad4-c11^{TopBP1}:GFP* cells. The Rad9 immunoprecipitates were then probed by immunoblotting with mouse anti-HA (12CA5). Coprecipitation of Rad9:HA with Rad4^{TopBP1}:GFP or Rad4-c11^{TopBP1}:GFP was detected by rabbit anti-GFP (Abcam, Cambridge, United Kingdom). The two arrows marked with asterisks in Rad4^{TopBP1}:GFP immunoprecipitation denote full-length and N-terminal truncation of the Rad4^{TopBP1} protein. IgG was used as control of the immunoprecipitation. α-tubulin or Cdc2 (PSTAIRE) were used as input loading control.

Rad4^{TopBP1} Protein Associates with Checkpoint Sensor Proteins and Mutation in rad4-c11^{TopBP1} Reduces the Mutant's Rad9 Phosphorylation

Chk1 activation in response to DNA damage depends on the checkpoint complexes, Rad3^{ATR}-Rad26^{ATRIP}, Rad9-Rad1-Hus1, Rad17-Rfc$_{2-5}$, and Rad4^{TopBP1} (O'Connell and Cimprich, 2005). A recent study has shown that association of Rad4^{TopBP1} with a phosphorylated form of Rad9 is required to promote Chk1 activation (Furuya *et al.*, 2004). Given that the mutation in *rad4-c11^{TopBP1}* compromises Chk1 phosphorylation in response to CPT-induced damage (Figures 2 and 3), we examined the physical association of Rad4^{TopBP1} or Rad4-c11^{TopBP1} protein with all of the checkpoint sensor proteins, with or without CPT treatment. Wild-type and mutant Rad4^{TopBP1}:GFP protein were detected in the anti-Rad26^{ATRIP} immunoprecipitates from extracts of *rad4$^{+TopBP1}$:GFP* and *rad4-c11^{TopBP1}:GFP* cells (Figure 4A). Rad3^{ATR}:myc was detected in the anti-GFP immunoprecipitates from extracts of *rad4$^{+TopBP1}$:GFP rad3^{+ATR}:myc* and *rad4-c11^{TopBP1}:GFP rad3^{+ATR}:myc* cells after either CPT or HU treatment (Figure 4B). In contrast to that reported in Furuya *et al.* (2004), no significant increased level of Rad3^{ATR} associated with either Rad4^{TopBP1} or Rad4-c11^{TopBP1} was detected after treatment with these genotoxic agents (Figure 4B). The discrepancy may due to the damaged structures induced by these genotoxic agents being different from those induced by γ-radiation used by Furuya *et al.* Furthermore, Hus1:myc and Rad17:myc were detected in the GFP immunoprecipitates from cell extracts of *rad4$^{+TopBP1}$:GFP hus1^{+}:myc, rad4-c11^{TopBP1}:GFP hus1^{+}:myc* (Figure 4C), and *rad4$^{+TopBP1}$:GFP rad17^{+}:myc* and *rad4-c11^{TopBP1}:GFP rad17^{+}:myc* cells (Figure 4D). These results indicate that Rad4^{TopBP1} associates with Rad3^{ATR}-Rad26^{ATRIP}, Hus1, and the clamp loader Rad17 in vivo, independent of damage, thus suggesting that Rad4^{TopBP1} physically coexists with these checkpoint sensor proteins in a complex. Importantly, the mutation in *rad4-c11^{TopBP1}* does not affect the association of mutant Rad4-c11^{TopBP1} protein with Rad3^{ATR} -Rad26^{ATRIP}, Hus1, Rad9, and Rad17 checkpoint sensor proteins. Hence, failure to activate the Chk1 damage checkpoint in *rad4-c11^{TopBP1}* is not due to the inability of Rad4-c11^{TopBP1} to associate with checkpoint sensor proteins.

It has been shown that Chk1 phosphorylation in response to DNA damage requires the interactions of R3 and R4 domains of Rad4^{TopBP1} with the Rad9 protein phosphorylated at Thr^{412}/Ser^{423} (T412/S423), which then promotes the coprecipitation of Rad4^{TopBP1} with Rad3^{ATR} in coordinating the formation of an active checkpoint complex (Furuya *et al.*, 2004). Because *rad4-c11^{TopBP1}* mutant harboring a mutation in R3 domain has defective Chk1 damage checkpoint (Figures 2 and 3), we investigated whether the Rad4-c11^{TopBP1} is able to interact with Rad9 by two-hybrid assay and by coimmunoprecipitation. We constructed *rad9^{+}* as bait and *rad4$^{+TopBP1}$* or *rad4-c11^{TopBP1}* with a deletion of the R1 and R2 domains (ΔR1R2Rad4^{TopBP1} or ΔR1R2Rad4-c11^{TopBP1} in Figure 4E) as targets and estimated the interactions by measuring the β-galactosidase activity. Rad9 interacted with ΔR1R2Rad4^{TopBP1} (Figure 4E) to a extent comparable to that of the full-length Rad4^{TopBP1} (unpublished data). In contrast, the interaction between ΔR1R2Rad4-c11^{TopBP1} and Rad9 was reduced about fourfold, but not abolished (Figure 4E). Thus, the E368K substitution in the Rad4-c11^{TopBP1} protein adversely affects the interaction between these two proteins.

To confirm this observed interaction in vivo, we examined coimmunoprecipitation of Rad9 with Rad4^{TopBP1}. In either asynchronous cells or CPT-treated cells, Rad4^{TopBP1} and Rad4-c11^{TopBP1} proteins were detected in the anti-HA-Rad9 immunoprecipitates, thus supporting the two-hybrid finding that mutation in *rad4-c11^{TopBP1}* does not abolish the association of Rad4-c11^{TopBP1} mutant protein with Rad9 (Figure 4F, lanes 1–4). Furuya *et al.* (2004) have also shown that Rad9 phosphorylated at Thr^{225} (T225) results in a slow mobility form of Rad9 protein in gel and that the Rad9-T225 phosphorylation is dependent on the prior phosphorylation at Rad9-T412/S423. Upon CPT treatment, the Rad9-T225 phosphorylation was substantially reduced in *rad4-c11^{TopBP1}* (Figure 4F, compare lane 2 with lane 4). These results support the notion proposed by Furuya *et al.* that phosphorylations of Rad9 at T412/S423 promote the interaction of Rad4^{TopBP1} with Rad9 and Rad3^{ATR} and the interaction is required to activate Chk1 damage checkpoint.

The Mutation in rad4-c11^{TopBP1} Does Not Affect DNA Replication or Cell Cycle Progression

The association of budding yeast Pol1$^{Pol\alpha}$ and Pol2$^{Pol\varepsilon}$ to the origin of DNA replication is thought to require Dpb11^{TopBP1}, and this association functions mainly during initiation of DNA replication (Araki *et al.*, 1995; Masumoto *et al.*, 2000). However, human TopBP1 has been shown to associate with Polε throughout the cell cycle (Makiniemi *et al.*, 2001). Finding that the *rad4-c11^{TopBP1}* mutation compromises the cells' Chk1 damage checkpoint response prompted us to test whether this mutation had effects on the replication function of Rad4^{TopBP1} and cell cycle progression.

We first examined the physical association of Rad4^{TopBP1} and mutant Rad4-c11^{TopBP1} proteins with the replicative DNA polymerases, Polα, Polε, and Polδ. Immunoprecipitates of anti-GFP of GFP-tagged Rad4^{TopBP1} and Rad4-c11^{TopBP1} proteins from extracts of *rad4$^{+TopBP1}$:GFP* or *rad4-c11^{TopBP1}:GFP* cells harboring either *polδ^{+}:Flag* or *polε^{+}:Flag* were probed for coprecipitation of Polδ or Polε using an anti-Flag antibody (Figure 5A). Flag-tagged Polδ and Polε proteins were detected in the GFP immunoprecipitates from extract of asynchronous cells and HU- or CPT-treated cells expressing the GFP-tagged Rad4^{TopBP1} or Rad4-c11^{TopBP1} (Figure 5A). Similarly, GFP-tagged Rad4^{TopBP1} or Rad4-c11^{TopBP1} was detected in Polα-immunoprecipitates from cell extracts of either *rad4$^{+TopBP1}$:GFP* or *rad4-c11^{TopBP1}:GFP* (Figure 5B). These results indicate that Rad4^{TopBP1} associates with all three replicative polymerases in a protein complex not only during initiation of DNA replication but also in predominantly G2 phase of the fission yeast cell cycle. Importantly, the mutation in *rad4-c11^{TopBP1}* does not affect the Rad4-c11^{TopBP1} protein's ability to associate with the replicative polymerases in the complex. Thus, failure to activate Chk1 damage checkpoint in *rad4-c11^{TopBP1}* is not due to the inability of Rad4-c11^{TopBP1} protein to associate with the replicative polymerases.

To further confirm that the failure to activate Chk1 in response to DNA damage in *rad4-c11^{TopBP1}* is not due to an S-phase defect, we investigated whether this mutation affects cell cycle progression by monitoring Cdc2 phosphorylation. *rad4-c11^{TopBP1}:GFP cdc25-22* as well as *rad4$^{+TopBP1}$:GFP cdc25-22* were blocked in G2 at 36.5°C and then released into the cell cycle at 26°C. Samples were removed every 20 min to analyze the phosphorylation of Cdc2 protein and to measure the septation index. After release from G2 arrest by *cdc25-22*, both *rad4$^{+TopBP1}$:GFP cdc25-22* and *rad4-c11^{TopBP1}:GFP cdc25-22* had identical septation indices (SI%), which peaked at cytokinesis at ~60 min. Cdc2 phosphorylation in *rad4$^{+TopBP1}$:GFP cdc25-22* and *rad4-c11^{TopBP1}:GFP cdc25-22* were maximal during G2 arrest, and both strains exhibited a reduced Cdc2 phosphorylation after 60-min release from G2 arrest and progressed through the cell cycle in similar manner (Figure 5C). Thus, both genetic and biochemical evidence (Figure 5, A and B) as well as the cell cycle analysis (Figure 5C) indicate that mutation in *rad4-c11^{TopBP1}* does not affect the mutant's DNA replication and cell cycle progression.

Rad4-c11^{TopBP1} Protein Has Compromised Interaction with Crb3

We further explored what other protein–protein interactions that could be compromised by the *rad4-c11^{TopBP1}* mutation, which might explain the failure to activate the Chk1 damage checkpoint. Two-hybrid analysis using either the R1+R2 or the R3 domain of Rad4^{TopBP1} has previously identified the interactions with Crb2 and Crb3, respectively (Saka *et al.*, 1997). Fission yeast *crb3^{+}* is an essential gene, and its gene product is thought to be involved in the G1/S progression (Saka *et al.*, 1997). However, the biological significance of the interaction between the R3 domain of Rad4^{TopBP1} and Crb3 is unknown.

Given that the mutation in *rad4-c11^{TopBP1}* is in the R3 domain, we used two-hybrid analysis to examine whether this mutation had any adverse effects on the interaction of Rad4^{TopBP1} with Crb3. Both Crb3 and Chk1 interact with the R3 domain of Rad4^{TopBP1} as bait (Figure 6A). In striking contrast, both Crb3 and Chk1 failed to interact with the R3 domain of Rad4-c11^{TopBP1}. We also performed this analysis using *crb3^{+}* as bait and full-length *rad4$^{+TopBP1}$* or *rad4^{TopBP1}* containing a deletion of R1 and R2 domains (ΔR1R2rad4 in Figure 6B) as targets. Both full-length and ΔR1R2rad4 target constructs were proficient in interacting with Crb3. Again, the interaction between Crb3 and Rad4-c11^{TopBP1} with deletion of R1 and R2 motifs (ΔR1R2rad4-c11 in Figure 6B) was reduced to the same level as Crb3 by itself, which exhibited a low level of transactivation. Thus, the two-hybrid results confirm the previous report (Saka *et al.*, 1997) that the R3 domain of Rad4^{TopBP1} interacts with Crb3. Importantly, mutation in the R3 domain of *rad4-c11^{TopBP1}* significantly reduces the extent of interaction of Rad4-c11^{TopBP1} with Crb3 and Chk1 (Figure 6A).

To confirm the two-hybrid interaction, numerous attempts under various conditions to demonstrate copre-

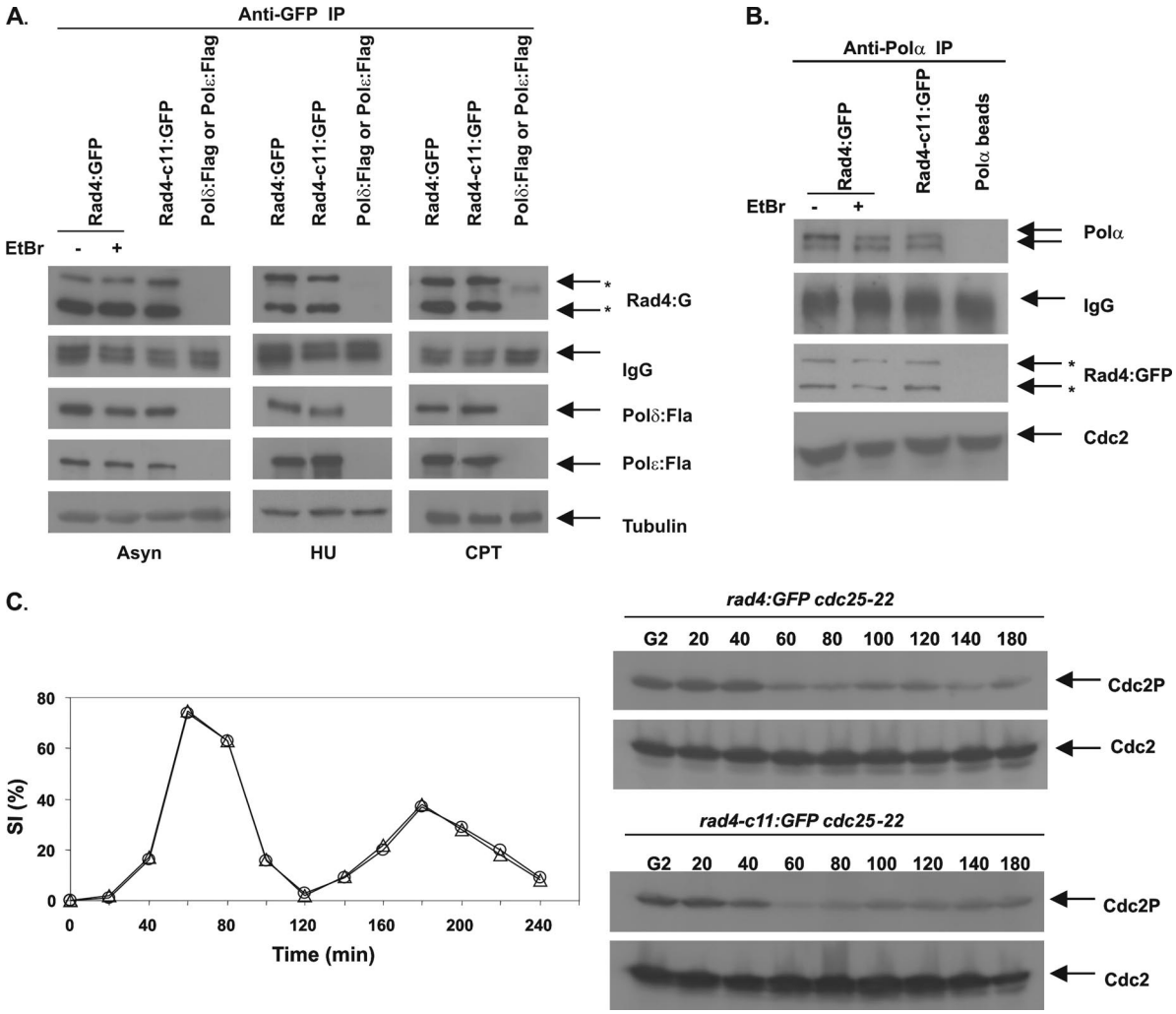

Figure 5. Association of Rad4^{TopBP1} and replicative DNA polymerases and mutation in r*ad4-c11^{TopBP1}* does not affect the association and cell cycle progression. (A) Coprecipitation of Rad4^{TopBP1}:GFP or Rad4-c11^{TopBP1}:GFP with Polδ and Polε. Cells with *polε^{+}:Flag* or *polδ^{+}:Flag* in *rad4$^{+TopBP1}$:GFP* or *rad4-c11^{TopBP1}:GFP* were grown in YES media and treated with either 30 μM CPT for 2 h or 12 mM HU for 4 h at 30°C. Cell extracts were immunoprecipitated with anti-GFP antibody and probed with anti-Flag antibody for coprecipitation of Polε:Flag or Polδ:Flag. (B) Coprecipitation of Rad4^{TopBP1}:GFP or Rad4-c11^{TopBP1}:GFP with Polα. Cell extracts of *rad4$^{+TopBP1}$:GFP* or *rad4-c11^{TopBP1}:GFP* were immunoprecipitated with anti-Polα antibody cross-linked onto Agarose beads, and the immunoprecipitates were probed with anti-GFP. The coprecipitations of the replicative DNA polymerases with Rad4^{TopBP1}or Rad4-c11^{TopBP1} were not caused by the presence of cellular DNA as shown in the ethidium bromide (EtBr) control. The two arrows marked with asterisks in Rad4^{TopBP1}:GFP immunoprecipitation denote full-length and N-terminal truncation of the Rad4^{TopBP1} protein. IgG was used as control of immunoprecipitation. α-tubulin or Cdc2 (PSTAIRE) were used as input loading control. (C) *rad4-c11^{TopBP1}* mutant has normal cell cycle progression. *rad4$^{+TopBP1}$:GFP cdc25-22* and *rad4-c11^{TopBP1}:GFP cdc25-22* cells were arrested in G2 at 36°C and released to mitosis by shift to 26°C. Cell extracts were prepared in every 20 min and analyzed for Cdc2 phosphorylation by immunoblotting with polyclonal antibodies to phospho-Cdc2 (Tyr15) and Cdc2 (PSTAIRE). *rad4$^{+TopBP1}$:GFP cdc25-22* (○) and *rad4-c11^{TopBP1}:GFP cdc25-22* (◇) cells were examined microscopically for the septation index (SI), and both wild-type and mutant cells exhibited identical septation index.

cipitation of Rad4^{TopBP1}:GFP and Crb3-Flag were unsuccessful. To eliminate the possible interference of coprecipitation by the Flag-tag on Crb3 and the possible transient nature of the interaction, we examined the Rad4^{TopBP1}:GFP associated proteins in the Rad4^{TopBP1}:GFP immunoprecipitates after CPT treatment by tandem mass spectrometric (MS/MS) analysis. In the Rad4^{TopBP1}:GFP immunoprecipitates, a faint protein band in SDS gel with molecular mass corresponding to Crb3 was identified among several Coomassie Blue–stained proteins. This band was dissected from the gel, trypsinized, and subjected to MS/MS analysis. The analyses revealed a peptide fragment having sequence, LYTASEDNTIR, matching the Crb3 protein sequence (Supplementary Figure 2A). In contrast, no protein species corresponding to the Crb3 molecular mass or protein sequence were identified among the Coomassie Blue–stained proteins of Rad4-c11^{TopBP1}:GFP immunoprecipitates after CPT treatment (Supplementary Figure 2B). Hence, these results suggest a weak or transient association between Rad4^{TopBP1} and Crb3, which is compromised in Rad4-c11^{TopBP1}.

We further investigated whether Crb3 interacts with Chk1 and Cds1 by two-hybrid assay. Crb3 interacted with both Cds1 and Chk1 by the two-hybrid criteria (Figure 6B). Confirmation of the two-hybrid results by coprecipitation of Flag-tagged Crb3 with Cds1 or HA-tagged Chk1 from cell

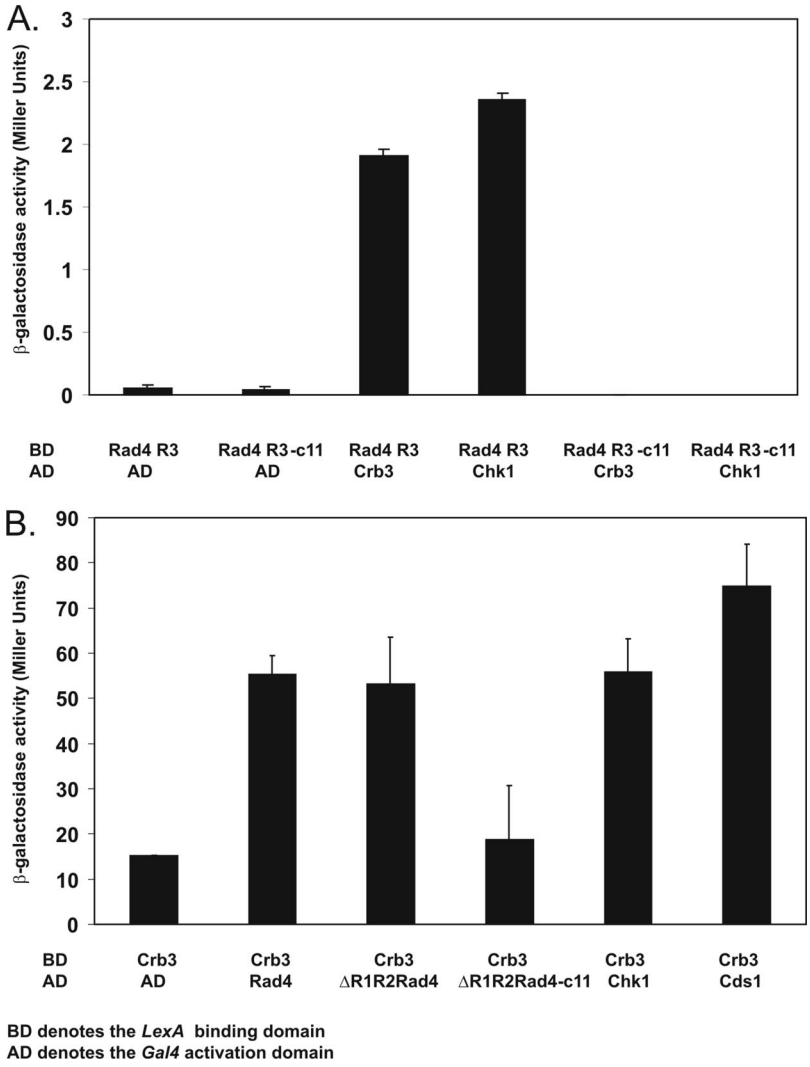

Figure 6. Two-hybrid assay of the interaction of wild-type Rad4^{TopBP1} or mutant Rad4-c11^{TopBP1} with Crb3. (A) R3 domain of Rad4^{TopBP1} interacted with Crb3 and Chk1 and Rad4-c11^{TopBP1} R3 domain failed to interact with both Crb3 and Chk1. Two-hybrid assay with Rad4^{TopBP1} R3 BRCT or Rad4-c11^{TopBP1} R3 BRCT domain as baits and Chk1 and Crb3 as targets. (B) Interaction of Crb3 with the Rad4^{TopBP1} C terminal region containing the R3R4 BRCT domains and with Chk1 and Cds1. Two-hybrid assay with full-length Crb3 as bait and ΔR1R2 Rad4^{TopBP1} and ΔR1R2 Rad4-c11^{TopBP1} as targets were performed as described in *Materials and Methods.* ΔR1R2 represents the construct with the deletion of R1R2 BRCT domains of *rad4$^{+TopBP1}$*.

extracts were inconclusive due to the background affinity of Crb3 for the immuno-affinity matrix.

Crb3 Has a Role in Maintaining the Chk1 Damage Checkpoint Response

To determine whether Crb3 has a role in the Chk1 checkpoint response, we characterized *crb3$^+$*. A strain, *crb3::ura4* (Δ*crb3*) in which the entire coding region of *crb3$^+$* gene was replaced by *ura4$^+$* was not viable, confirming that *crb3$^+$* is an essential gene (Saka *et al.,* 1997). We then investigated the role of *crb3$^+$* in checkpoint response and in cell viability by generating mutants of *crb3$^+$* using both PCR random mutagenesis and hydroxylamine mutagenesis. Surprisingly, all of the mutants generated by either method reverted back to wild type in exceedingly high frequency.

To circumvent this difficulty, we constructed diploid strains of homozygous mating type. Diploid *chk1:HA* Δ*crb3*/+ cells with one copy of the *crb3$^+$* gene deleted were tested for their sensitivity to treatment using 10 μM CPT or 5 mM HU on solid media at 30°C. Cells having a single copy of *crb3$^+$* exhibited higher sensitivity to CPT and HU treatment than wild type (Figure 7A), suggesting that cells with a lower *crb3$^+$* gene dose are more sensitive to DNA damage.

HU treatment inhibits cells' ribonucleotide reductase (RNR), thus resulting in replication fork stalling due to depletion of cellular deoxyribonucleotide pool (Reichard, 1988). Studies of budding yeast have demonstrated that prolonged HU exposure of cells results in the recruitment of Mre11 and Rad52 to process the DNA breaks and initiate recombination in order to facilitate replication fork restart (Lisby *et al.,* 2004). Thus, this study has demonstrated a convincing experimental evidence that chronic HU treatment causes DNA damage, possibly because of replication fork collapse (Lisby *et al.,* 2004; Lisby and Rothstein, 2004). To further determine whether *crb3$^+$* is required for DNA damage response induced by chronic HU treatment, we analyzed the DNA damage checkpoint response of diploid cells containing a single copy of Δ*crb3* by quantifying the mitotic catastrophic phenotype of cells after HU treatment. Diploid strains were incubated for 4, 8, and 10 h in culture containing 12 mM HU (Figure 7B). After 10 h of HU treatment, 15% of wild-type (+/+) diploid cells exhibited a mitotic catastrophic phenotype. Δ*crb3*/+ diploid with one copy of intact *crb3$^+$* and *rad4-c11^{TopBP1}*/+ diploid with one copy of intact *rad4$^{+TopBP1}$* exhibited ~20% of the cells entering catastrophic mitosis, which were comparable to the wild-type cells. Approximately 35 and 62% of the *+rad4-c11^{TopBP1}*/*+rad4-c11^{TopBP1}* diploid cells having both copies of *rad4-c11^{TopBP1}* mutation exhibited a mitotic catastrophic phenotype after 8 and 10 h of HU treatment, respectively

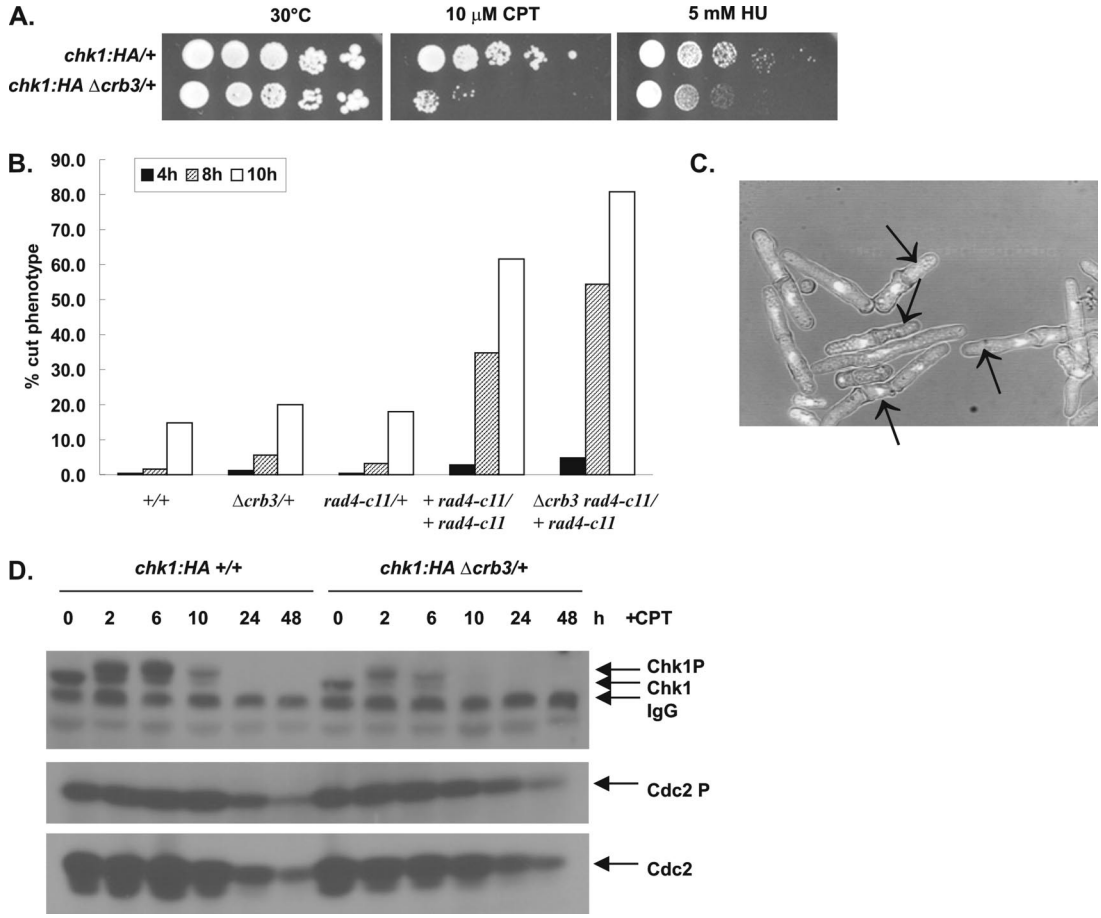

Figure 7. Effects of *crb3*$^{+}$ gene dose on the DNA damage checkpoint response. (A) Lower *crb3*$^{+}$ gene dose enhances cells' sensitivity to CPT and HU. Diploid cells (1×10^7) of *chk1:HA* +/+ (diploid with two copies of wild-type *crb3*$^{+}$) and *chk1:HA* Δ*crb3*/+ (diploid with one copy of Δ*crb3*) were cultured to log phase, then 10-fold serial diluted, and spotted onto YES plates or plates with 10 μM CPT or 5 mM HU, followed by incubating at 30°C for 3 d. (B) Diploid wild type (+/+, with two copies of wild-type *crb3*$^{+}$), Δ*crb3*/+ (diploid cells with one copy of the *crb3*$^{+}$ deletion), *rad4-c11*^{TopBP1}/+ (diploid cells with one copy *rad4-c11*^{TopBP1} mutation), +*rad4-c11*^{TopBP1}/+*rad4-c11*^{TopBP1} (diploid cells with both copies of *rad4-c11*^{TopBP1} mutation, but two copies of wild-type *crb3*$^{+}$), and Δ*crb3 rad4-c11*^{TopBP1}/+*rad4-c11*^{TopBP1} (diploid cells with one copy of *crb3*$^{+}$ deletion and both copies of *rad4-c11*^{TopBP1} mutation) were grown in YES media with 12 mM HU for the indicated times at 30°C, fixed, and stained with DAPI to score cells' % *cut* phenotype. Percentage of *cut* phenotype represents the average of two independent experiments of counting 300 cells per experiment. Percentage difference between the two independent points is <2.5%. (C) Fluorescence microscopy of DAPI-stained Δ*crb3 rad4-c11*^{TopBP1}/+ *rad4-c11*^{TopBP1} diploid cells after incubating in 12 mM HU for 10 h at 30°C. Arrows indicate the cells exhibiting abnormal nuclei. (D) Diploids with deletion of one copy of the *crb3*$^{+}$ compromise the maintenance of CPT-induced Chk1 phosphorylation and Chk1 protein stability. Strains *chk1:HA* +/+ (diploid with HA-tagged *chk1*$^{+}$ and both copies of wild-type *crb3*$^{+}$) and *chk1:HA* Δ*crb3*/+ (diploid with HA-tagged *chk1*$^{+}$ and one copy of *crb3*$^{+}$ deleted) were grown in YES in the presence of 30 μM CPT and incubated for 2, 6, 10, 24, and 48 h at 30°C. Chk1:HA protein was immunoprecipitated from extracts with 4 μl of rat anti-HA and protein G plus Agarose beads. Chk1 proteins were detected by immunoblotting with mouse anti-HA (12CA5). Immunoblotting of Cdc2 phosphorylation with anti-phospho-Cdc2 (Tyr15) and anti-Cdc2 (PSTAIRE) were used as an input control.

(Figure 7B), again confirming the requirement of *rad4-c11*^{TopBP1} for maintaining the DNA damage checkpoint response to chronic HU treatment. Significantly, 55 and 81% of the Δ*crb3 rad4-c11*^{TopBP1}/+*rad4-c11*^{TopBP1} cells, which contain only one copy of the intact *crb3*$^{+}$ and both copies of *rad4-c11*^{TopBP1} mutation, entered catastrophic mitosis after 8 and 10 h HU treatment, respectively. After 10 h of HU treatment, these cells exhibited various mitotic catastrophic phenotypes (Figure 7C). Thus, reduction of the *crb3*$^{+}$ gene dosage indeed compromises the chronic HU treatment induced damage checkpoint activation. Furthermore, reduction of *crb3*$^{+}$ gene dosage and the mutation in *rad4-c11*^{TopBP1} cause an additive effect on DNA damage checkpoint response (Figure 7B), suggesting that Crb3 may be involved in a separate damage response pathway from the Rad4^{TopBP1} dependent pathway, which may influence the role of Rad4^{TopBP1} in damage checkpoint.

To further investigate the role of *crb3*$^{+}$ in Chk1 damage checkpoint activation, we analyzed the Chk1 phosphorylation in *chk1:HA* Δ*crb3*/+ cells containing one copy of intact *crb3*$^{+}$ and compared with *chk1:HA* +/+ cells with both copies of *crb3*$^{+}$. On CPT treatment, Chk1 protein in the *chk1:HA* +/+ cells was phosphorylated and remained phosphorylated up to 10 h. In the *chk1:HA* Δ*crb3*/+ cells, the level of Chk1 protein was slightly reduced, suggesting that Chk1 also might be unstable in cells with lower *crb3*$^{+}$ gene dosage. Furthermore, the CPT-induced Chk1 phosphorylation was maintained only for 6 h with no detectable Chk1 after 10 h (Figure 7D). Taken together, these results suggest that Crb3 has a role in the maintenance of Chk1 activation when DNA is dam-

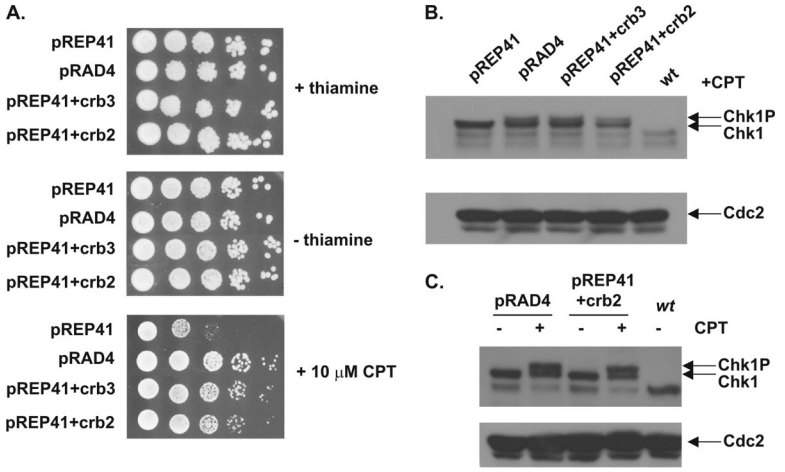

Figure 8. Expression of *crb3*$^+$ restores DNA damage checkpoint response in *rad4-c11*^{TopBP1}. (A) Expression of *crb3*$^+$ suppresses the CPT sensitivity of *rad4-c11*^{TopBP1}. *rad4-c11*^{TopBP1} strain was independently transformed with plasmids, *pREP41* (empty vector control), *prad4*$^{+TopBP1}$ (positive control), *pREP41:crb3*$^+$, and *pREP41:crb2*$^+$. Transformants (1×10^7) were serial diluted (1:10), spotted on media with or without thiamine to repress or activate the gene expression, respectively, and incubated at 30°C. The plates containing CPT did not contain thiamine. (B) Expression of *crb3*$^+$ or *crb2*$^+$ restores Chk1-mediated damage checkpoint in *rad4-c11*^{TopBP1}. Chk1:HA was immunoprecipitated from extracts of *rad4-c11*^{TopBP1} *chk1:HA* cells harboring either *prad4*$^{+TopBP1}$, *pREP41:crb3*$^+$, and *pREP41:crb2*$^+$ and analyzed for Chk1:HA phosphorylation by gel electrophoresis. (C) Restoration of Chk1 phosphorylation in *rad4-c11*^{TopBP1} is a specific response to DNA damage. Expression of *pREP41:crb2*$^+$ or *prad4*$^{+TopBP1}$ in undamaged *rad4-c11*^{TopBP1} did not induce Chk1 phosphorylation, whereas DNA damaged by CPT treatment-induced Chk1 phosphorylation in these cells. Cdc2 (PSTAIRE) was used as input control in all experiments.

aged and may also have a role in maintaining Chk1 protein stability.

Expression of crb3$^+$ *Suppresses the DNA Damage Checkpoint Defect and Restores Chk1 Activation in rad4-c11*^{TopBP1}

Finding that deletion of one copy of the *crb3*$^+$ in *rad4-c11*^{TopBP1}*/rad4-c11*^{TopBP1} exacerbates the damage checkpoint defect in cells prompted us to further investigate whether Crb3 influences the role of Rad4 in Chk1 damage checkpoint. We tested whether increasing the *crb3*$^+$ gene dose by ectopic expression of *crb3*$^+$ could suppress the CPT sensitivity of *rad4-c11*^{TopBP1}. Because activation of the Chk1 DNA damage checkpoint response depends on *crb2*$^+$ (Saka *et al.*, 1997; Mochida *et al.*, 2004), *crb2*$^+$ expression was used as a control. The cDNAs of *crb3*$^+$ and *crb2*$^+$ were independently constructed into the thiamine-regulated *pREP41* vector (Maundrell, 1993) to express in the *rad4-c11*^{TopBP1}. Empty *pREP41* vector and *prad4*$^{+TopBP1}$ expressed from its endogenous promoter were used as negative and positive controls, respectively, in *rad4-c11*^{TopBP1}. Cells were first grown in minimal media with thiamine and then without thiamine to induce the gene expression for 20 h. Mutant *rad4-c11*^{TopBP1} was sensitive to 10 μM CPT. Expression of *prad4*$^{+TopBP1}$ from its endogenous promoter suppressed this sensitivity (Figure 8A). Significantly, moderate expression of *crb3*$^+$ was capable in suppressing the CPT sensitivity of *rad4-c11*^{TopBP1}, indicating that an increase of *crb3*$^+$ gene dose can somehow suppress the Chk1 damage checkpoint defect in *rad4-c11*^{TopBP1} (Figure 8A). Interestingly, expression of *crb2*$^+$ was also able to suppress the *rad4-c11*^{TopBP1} CPT sensitivity, albeit to a slightly lesser extent than expression of *crb3*$^+$. These genetic results suggest that although Crb2 and Crb3 associate with different BRCT domains of Rad4^{TopBP1}, the associations have a mutual influence on the function of Rad4^{TopBP1} in the DNA damage checkpoint.

To ensure that the suppression of *rad4-c11*^{TopBP1} sensitivity to CPT by moderate expression of *crb2*$^+$ or *crb3*$^+$ is due to an enforcement of Chk1 activation, we compared the phosphorylation of Chk1 in *rad4-c11*^{TopBP1} transformed with the *pREP41* empty vector or *pREP41-crb3*$^+$, *pREP41-crb2*$^+$, and *prad4*$^{+TopBP1}$. Significantly, expression of *rad4*$^{+TopBP1}$, *crb3*$^+$, or *crb2*$^+$ in *rad4-c11*^{TopBP1} restored Chk1 phosphorylation after CPT treatment, whereas expression of empty vector did not (Figure 8B). To make certain that the restoration of Chk1 phosphorylation by the expression of either *crb2*$^+$ or *crb3*$^+$ is a response to CPT-induced damage not due to the overexpression, we expressed *crb2*$^+$ or *crb3*$^+$ in undamaged cells. Expression of *crb2*$^+$ or *crb3*$^+$ did not induce Chk1 phosphorylation in *rad4-c11*^{TopBP1} in undamaged cells (Figure 8C and unpublished data). These results thus indicate that both Crb3 and Crb2 function downstream of Rad4^{TopBP1} to activate Chk1 in response to the CPT damage-signaling pathway.

DISCUSSION

Studies of fission and budding yeasts have established that Rad4^{TopBP1} plays an essential role in both replication and checkpoint responses (Saka and Yanagida, 1993; Araki *et al.*, 1995; Masumoto *et al.*, 2000). In an effort to understand how Rad4^{TopBP1}, a single protein, can accomplish its multiple tasks, we identified four novel mutants of *rad4*$^{+TopBP1}$. One mutant, *rad4-c11*^{TopBP1}, harboring an E368K substitution in the R3 domain within the conserved motif (W-X-X-X-C/S) in all BRCT domains identified, enabled us to assess the roles of Rad4^{TopBP1} in checkpoint and replication, separately. A previous study of the thermosensitive mutant *rad4-116*^{TopBP1} has shown that at its semipermissive temperature of 32°C, the mutant has viability similar to that of the wild-type cells, but loses viability after 4 h in HU, showing *cut*-like cells within the population after 8 h in HU. These results thus imply that the *rad4-116*^{TopBP1} mutant lacks a DNA-replication checkpoint but not a compromised replication (McFarlane *et al.*, 1997). This study and others of the *rad4-116*^{TopBP1}, however, have not been able to definitively and thoroughly separate the role of Rad4^{TopBP1} in checkpoint responses from DNA replication by both biochemical and genetic approaches. Thus, it has been generally accepted that the roles of Rad4^{TopBP1} in checkpoint and DNA replication are linked. The *rad4-c11*^{TopBP1} mutant described in this study is defective in Chk1 activation in response to DNA damage but proficient in Cds1 activation in replication checkpoint response, DNA replication, and cell cycle progression. These results thus suggest that the acidic residue Glu^{368} plays a unique role in Chk1 activation in response to DNA damage. Thus, the role of Rad4^{TopBP1} in damage checkpoint response

can be separated from its roles in checkpoint response to replication perturbation and its role in DNA replication.

How Might the Mutation in rad4-c11^{TopBP1} Compromise the Chk1 Damage Checkpoint Response?

Rad4^{TopBP1} interacts with two proteins, Crb2 and Crb3, via the R1+R2 and R3 domains, respectively (Saka *et al.*, 1997). Activation of Chk1 in response to damage requires Crb2 (Mochida *et al.*, 2004). In *rad4-c11^{TopBP1}* mutant, it is possible that the structural alteration in the R3 domain due to the E368K substitution affects the structure of R1 domain, resulting in a weakening of the interaction with Crb2 and compromising the Chk1 damage checkpoint response. Our finding that expression of *crb2$^+$* can restore the Chk1 activation defect in *rad4-c11^{TopBP1}* supports this premise. A recent report has described that a *crb2* mutant that is defective in Chk1 activation is able to delay the metaphase to anaphase transition via a Mad2-dependent manner when cells are exposed to CPT treatment (Collura *et al.*, 2005). Given that deletion of *chk1$^+$* in *rad4-c11^{TopBP1}* has a synergistic effect in cells sensitivity to chronic CPT treatment, it is possible that the defect of *rad4-c11^{TopBP1}* mutation on Crb2 interaction may also compromise the Chk1-induced activation of the Mad2 -mediated spindle checkpoint to delay metaphase to anaphase transition.

Our results suggest that the mutation in *rad4-c11^{TopBP1}* also compromises the transient interaction between Rad4^{TopBP1} mutant protein with Crb3. Deletion of one copy of the *crb3$^+$* in diploid cells sensitizes the cells to CPT damage and compromises Chk1 maintenance. These results suggest that Crb3 has a role in Chk1 damage checkpoint. Notably, deletion of one copy of *crb3$^+$* gene in *rad4-c11^{TopBP1}/+ rad4-c11^{TopBP1}* diploid exacerbated the cells' damage checkpoint defect after prolonged HU treatment; moderate expression of *crb3$^+$* restores the *rad4-c11^{TopBP1}* mutant's Chk1 damage checkpoint response. Given the fact that Crb3 has a role in maintaining Chk1 activation and the association of Rad4^{TopBP1} and Crb3 is significantly reduced in *rad4-c11^{TopBP1}* and taking together all these findings, it is plausible that Crb3 affects the role of Rad4^{TopBP1} in Chk1 damage checkpoint. However, it is not yet known how the compromised interaction between Crb3 and Rad4-c11^{TopBP1} could affect the Chk1 damage defect observed in *rad4-c11^{TopBP1}*.

A recent study has shown that Chk1 activation in response to damage depends on association of Rad9 phosphorylated at T412/S423 with the R3 and R4 domains of Rad4^{TopBP1} and that this association promotes coprecipitation of Rad3^{ATR} with Rad4^{TopBP1}. These findings suggest that a prerequisite for the organization of the checkpoint apparatus is phosphorylation of specific checkpoint proteins; checkpoint activation is a consequence of the interactions between the phospho-specific proteins (Furuya *et al.*, 2004). Consistent with such a model, we show here that the level of phosphorylation of Rad9 protein at T225 is reduced in *rad4-c11^{TopBP1}* in response to CPT-induced damage. As shown by Fuyura *et al.* (2004) phosphorylation at T225 of Rad9 depends on its prior phosphorylations at T412/S423. Thus, the decreased phosphorylation of Rad9-T225 reflects a reduced level of phosphorylation of Rad9 at T412/S423. Hence this could be another possible cause of the Chk1 damage response defect in *rad4-c11^{TopBP1}*.

Recent studies of TopBP1 in *Xenopus* egg extracts and human cells have shown that TopBP1 is a positive effector of ATR by stimulating the kinase activity of ATR for initiation of the ATR-dependent signaling processes in checkpoint responses (Kumagai *et al.*, 2006). Rad4^{TopBP1} of fission yeast associates with Rad3^{ATR}-Rad26^{ATRIP} and the *rad4^{TopBP1}-c11* mutation does not compromise the physical association between these proteins. However, it is conceivable that although the Rad4^{TopBP1}-c11 mutant protein is able to associate with Rad3^{ATR}-Rad26^{ATRIP}, the *rad4^{TopBP1}-c11* mutation somewhat compromises the ability of the mutant Rad4^{TopBP1}-c11 protein to stimulate the kinase activity of Rad3^{ATR}, thus resulting in the Chk1 damage checkpoint defect.

Rad4^{TopBP1} Provides a Scaffolding Framework Linking Replication with the Checkpoint to Maintain Genomic Integrity

We show here that Rad4^{TopBP1} physically associates with the checkpoint sensors and replicative polymerases, and transiently associates with Crb2 and Crb3. The three replicative polymerases, α, δ, and ε, have been shown to localize and function together at replication fork throughout the cell cycle in *S. cerevisiae* (Hiraga *et al.*, 2005). Findings that Rad4^{TopBP1} associates with all three replicative polymerases not only during DNA replication but also during the predominately G2 phase of the fission yeast cell cycle suggests that Rad4^{TopBP1} is an integral component of a protein complex at the replication fork throughout the cell cycle. The replicative polymerases are also involved in DNA repair (Holmes and Haber, 1999; Wang *et al.*, 2004). Associations of Rad4^{TopBP1} with these polymerases and checkpoint sensor proteins in G2 cells suggest that Rad4^{TopBP1} may also have a role in coordinating these proteins for DNA repair.

Analyses of the four novel *rad4^{TopBP1}* mutants show that these mutants have distinct and overlapping phenotypes. Notably, *rad4-116^{TopBP1}* and *rad4-c23^{TopBP1}* harboring amino acid substitutions in adjacent residues Thr^{45} and His^{46}, respectively, have distinct phenotypes. These findings suggest that residues in each BRCT-domain of Rad4^{TopBP1} could interact with different partners to enforce checkpoint response or replication. Our results in this study led us to propose that Rad4^{TopBP1} serves as a scaffold to a large protein complex containing both replication proteins and checkpoint proteins. By means of its many interacting partners, Rad4^{TopBP1} functions in the checkpoint machinery to monitor the genomic status and selectively activate checkpoint responses to DNA damage or replication perturbation during the cell cycle.

ACKNOWLEDGMENTS

We thank A. M. Carr and K. Furuya for *rad9$^+$:HA* strain. This work is supported by grants from the National Cancer Institute of the National Institutes of Health.

REFERENCES

Araki, H., Leem, S. H., Phongdara, A., and Sugino, A. (1995). Dpb11, which interacts with DNA polymerase II(epsilon) in *Saccharomyces cerevisiae*, has a dual role in S-phase progression and at a cell cycle checkpoint. Proc. Natl. Acad. Sci. USA *92*, 11791–11795.

Bahler, J., Wu, J. Q., Longtine, M. S., Shah, N. G., Mckenzie, A., III, Steever, A. B., Wach, A., Philippsen, P., and Pringle, J. R. (1998). Heterologous modules for efficient and versatile PCR-based gene targeting in *Schizosaccharomyces pombe*. Yeast *14*, 943–951.

Bakkenist, C. J., and Kastan, M. B. (2004). Initiating cellular stress responses. Cell *118*, 9–17.

Boddy, M. N., Furnari, B., Mondesert, O., and Russell, P. (1998). Replication checkpoint enforced by kinase Cds1 and Chk1. Science *280*, 909–912.

Collura, A., Blaisonneau, J., Baldacci, G., and Francesconi, S. (2005). The fission yeast Crb2/Chk1 pathway coordinates the DNA damage and spindle checkpoint in response to replication stress induced by topoisomerase I inhibitor. Mol. Cell. Biol. *25*, 7889–7899.

Furuya, K., Poitelea, M., Guo, L., Caspari, T., and Carr, A. M. (2004). Chk1 activation requires Rad9 S/TQ-site phosphorylation to promote association with C-terminal BRCT domains of Rad4^{TOPBP1}. Genes Dev. *18*, 1154–1164.

Garcia, V., Furuya, K., and Carr, A. M. (2005). Identification and functional analysis of TopBP1 and its homologs. DNA Repair (Amst) *4*, 1227–1239.

Griffiths, D., Uchiyama, M., Nurse, P., and Wang, T.S.-F. (2000). A novel allele of the chromatin-bound fission yeast checkpoint protein Rad17 separates the DNA structure checkpoints. J. Cell Sci. *113*, 1075–1088.

Gyuris, J., Golemis, E., Chertkov, H., and Brent, R. (1993). Cdi1, a human G1 and S phase protein phosphatase that associates with Cdk2. Cell *75*, 791–803.

Harris, S., Kemplen, C., Caspari, T., Chan, C., Lindsay, H. D., Poitelea, M., Carr, A. M., and Price, C. (2003). Delineating the position of *rad4*$^{+}$/*cut5*$^{+}$ within the DNA-structure checkpoint pathways in *Schizosaccharomyces pombe.* J. Cell Sci. *35*, 3519–3529.

Hiraga, S., Hagihara-Hayashi, A., Ohya, T., and Sugino, A. (2005). DNA polymerases alpha, delta, and epsilon localize and function together at replication forks in *Saccharomyces cerevisiae.* Genes Cells *10*, 297–309.

Holmes, A. M., and Haber, J. E. (1999). Double-strand break repair in yeast requires both leading and lagging strand DNA polymerases. Cell *96*, 415–424.

Kastan, M. B., and Bartek, J. (2004). Cell-cycle checkpoints and cancer. Nature *432*, 316–323.

Killian, D. J., and J. Hubbard, E. (2004). *C. elegans* pro-1 activity is required for soma/germline interactions that influence proliferation and differentiation in the germ line. Development *6*, 1267–1278.

Kumagai, A., Lee, J., Yoo, H. Y., and Dunphy, W. G. (2006). TopBP1 activates the ATR-ATRIP complex. Cell *124*, 943–955.

Lindsay, H. D., Griffiths, D.J.F., Edwards, R., Murray, J. M., Christensen, P. U., Walworth, N., and Carr, A. M. (1998). S-phase specific activation of Cds1 kinase defines a subpathway of the checkpoint response in *S. pombe.* Genes Dev. *12*, 382–395.

Lisby, M., Barlow, J. H., Burgess, R. C., and Rothstein, R. (2004). Choreography of the DNA damage response; spatiotemporal relationships among checkpoint and Repair proteins. Cell *118*, 699–713.

Lisby, M., and Rothstein, R. (2004). DNA damage checkpoint and repair centers. Curr. Opin. Cell Biol. *16*, 328–334.

Lukas, J., and Bartek, J. (2004). Watching the DNA repair ensemble dance. Cell *118*, 666–668.

Makiniemi, M. *et al.* (2001). BRCT domain-containing protein TopBP1 functions in DNA replication and damage response. J. Biol. Chem. *276*, 30399–30406.

Masumoto, H., Sugino, A., and Araki, H. (2000). Dpb11 controls the association between DNA polymerases alpha and epsilon and the autonomously replicating sequence region of budding yeast. Mol. Cell. Biol. *20*, 2809–2817.

Maundrell, K. (1993). Thiamine-repressible expression vectors pREP and pRIP for fission yeast. Gene *123*, 127–130.

McFarlane, R. J., Carr, A. M., and Price, C. (1997). Characterisation of the *Schizosaccharomyces pombe rad4/cut5* mutant phenotypes: dissection of DNA replication and G2 checkpoint control function. Mol. Gen. Genet. *255*, 332–340.

Mochida, S., Esashi, F., Aono, N., Tamai, K., O'Connell, M. J., and Yanagida, M. (2004). Regulation of checkpoint kinases through dynamic interaction with Crb2. EMBO J. *23*, 418–428.

Moreno, S., Klar, A., and Nurse, P. (1991). Molecular genetic analysis of fission yeast *Schizosaccharomyces pombe.* Methods Enzymol. *194*, 795–823.

Nyberg, K. A., Michelson, R. J., Putnam, C. W., and Weinert, T. A. (2002). Toward maintaining the genome: DNA damage and replication checkpoints. Annu. Rev. Genet. *36*, 617–656.

O'Connell, M. J., and Cimprich, K. A. (2005). G2 damage checkpoints: what is the turn-on? J. Cell Sci. *118*, 1–6.

Park, H., Francesconi, S., and Wang, T. S. (1993). Cell cycle expression of two replicative DNA polymerases alpha and delta from Schizosaccharomyces pombe. Mol. Biol. Cell *4*, 145–157.

Perera, D., Perez-Hidalgo, L., Moens, P. B., Reini, K., Lakin, N., Syvaoja, J. E., San-Segundo, P. A., and Freire, R. (2004). TopBP1 and ATR colocalization at meiotic chromosomes: role of TopBP1/Cut5 in the meiotic recombination checkpoint. Mol. Biol. Cell *15*, 1568–1579.

Porter, S. E., and Champoux, J. J. (1989). Mapping in vivo topoisomerase I sites on simian virus 40 DNA: asymmetric distribution of sites on replicating molecules. Mol. Cell. Biol. *9*, 541–550.

Reichard, P. (1988). Interactions between deoxyribonucleotide and DNA synthesis. Annu. Rev. Biochem. *57*, 349–374.

Saka, Y., Esashi, F., Matsusaka, T., Mochida, S., and Yanagida, M. (1997). Damage and replication checkpoint control in fission yeast is ensured by interactions of Crb2, a protein with BRCT motif, with Cut5 and Chk1. Genes Dev. *11*, 3387–3400.

Saka, Y., Fantes, P., Sutani, T., McInerny, C., Creanor, J., and Yanagida, M. (1994a). Fission yeast *cut5* links nuclear chromatin and M phase regulator in the replication checkpoint control. EMBO J. *13*, 5319–5329.

Saka, Y., Fantes, P., and Yanagida, M. (1994b). Coupling of DNA replication and mitosis by fission yeast *rad4/cut5.* J. Cell Sci. (Suppl.) *18*, 57–61.

Saka, Y., and Yanagida, M. (1993). Fission yeast *cut5*$^{+}$, required for S phase onset and M phase restraint, is identical to the radiation-damage repair gene. rad4^{+}. Cell *74*, 383–393.

Swain, K. E., and Nurse, P. (1998). Regulation of cell polarity by microtubules in fission yeast. J. Cell Biol. *142*, 457–471.

Verkade, H. M., and O'Connell, M. J. (1998). Cut5 is a component of the UV-responsive DNA damage checkpoint in fission yeast. Mol. Gen. Genet. *260*, 426–433.

Walworth, N. C., and Bernards, R. (1996). Rad-dependent response of the chk1-encoded protein kinase at the DNA damage checkpoint. Science *271*, 353–356.

Wang, X., Ira, G., Tercero, J. A., Holmes, A. M., Diffley, J. F., and Haber, J. E. (2004). Role of DNA replication proteins in double-strand break-induced recombination in *Saccharomyces cerevisiae.* Mol. Cell. Biol. *24*, 6891–6899.